MIT Open Access Articles

Temporal Evolution of Surface Contamination under Ultra-high Vacuum

Massachusetts Institute of Technology

Temporal Evolution of Surface Contamination Under Ultra-High Vacuum

Zhen Liu,[1] Youngsup Song,[2,†] Anoop Rajappan,[1] Evelyn N. Wang,[2] Daniel J. Preston[1,*]

[1]Department of Mechanical Engineering, Rice University, 6100 Main St., Houston, TX 77006

[2]Department of Mechanical Engineering, Massachusetts Institute of Technology, 77 Massachusetts Ave., Cambridge, MA 02139

*To whom correspondence should be addressed: djp@rice.edu

ABSTRACT

Ultra-high vacuum (UHV) is essential to many surface characterization techniques and is often applied with the intention of reducing exposure to airborne contaminants. Surface contamination under UHV is not well-understood, however, and introduces uncertainty in surface elemental characterization or hinders surface-sensitive manufacturing approaches. In this work, we investigated the time-dependent surface composition of gold samples with different initial levels of contamination under UHV over a period of 24 hours with both experiments and physical modeling. Our results show that surface hydrocarbon concentration under UHV can be explained by molecular adsorption-desorption competition theory. Gold surfaces that were initially pristine adsorbed hydrocarbons over time under UHV; conversely, surfaces that were initially heavily contaminated desorbed hydrocarbons over time. During both adsorption and desorption, the concentration of contaminants tended toward the same equilibrium value. This study provides a comprehensive evaluation of the temporal evolution of surface contamination under UHV and highlights routes to mitigate surface contamination effects.

2

INTRODUCTION

Ultra-high vacuum (UHV) conditions are integral to a wide range of characterization techniques including X-ray photoelectron spectroscopy (XPS), scanning electron microscopy (SEM), low energy ion scattering, and even the Large Hadron Collider due to requirements for surface cleanliness and the unimpeded transmission of electron or ion beams.[1–4] Many of these techniques allow detailed surface morphology measurements or chemical composition analyses, enabling the quantitative study of thin films, interfaces, residues, and contamination for process development and control.[5–7] For instance, XPS has been critical for analysis of the chemical composition of carbon nitride,[8] graphene,[9,10] MXenes,[11] and rare earth oxides,[12] among other materials.

Surface science experiments often require chemically pristine sample surfaces without unwanted adsorbates, but it can be difficult to achieve clean surfaces in practice due to ubiquitous spontaneous contamination from the surrounding ambient environment. Volatile organic compounds (VOCs), typically hydrocarbons, represent a common surface contamination source which profoundly impacts surface composition and, in turn, affects wettability, adhesion, charge doping, carrier mobility, and other surface properties.[9] In fact, prior studies have reported time-dependent or inconsistent wetting behavior for a wide range of materials including graphene,[13–15] rare earth oxides,[16–18] silicon dioxide,[19] and metals and metal oxides,[20–24] generating confusion regarding intrinsic surface properties.

Ultra-high vacuum (i.e., pressures below 10^{-8} Torr)[25,26] may provide better control of contaminants; however, a limited understanding of the evolution of surface composition and effects of contamination persists even under well-regulated UHV conditions. In 1973, White

compared the contact angle of nichrome wafers before and after residence in a vacuum chamber for several hours and found that organic contamination occurs even under a high vacuum due to contaminants desorbed from the vacuum chamber walls, which are often exposed to the ambient air between experimental runs.[27] Desimoni and coworkers later found that prolonged storage in UHV can induce chemical modification of carbon fiber surfaces.[28] Martinez-Martin and colleagues also observed the adsorption of molecules on a sample surface inside of a vacuum chamber when studying the effect of atmospheric contaminants on graphitic surfaces.[29] Subsequently, Landoulsi and coworkers suggested that the contamination level of surfaces cleaned in ambient air cannot be accurately measured by XPS due to possible contamination inside the spectrometer; they reported that exposure to UHV may even lead to a faster rate of contamination, possibly due to the absence of adsorbed water or a more direct transfer of contaminant compounds.[30] Long and colleagues observed a similar phenomenon: a vacuum atmosphere accelerated the transition of laser-ablated copper from hydrophilic to hydrophobic.[31] Jagdheesh and coworkers even utilized high-vacuum storage intentionally to achieve a fast transition of wetting properties on laser-treated stainless steel.[32] Prakash and coworkers also experimentally characterized adsorption of hydrocarbon species under UHV in 2018, and they asserted that prior claims that storage under vacuum could prevent hydrocarbon contamination are wrong.[17,33] Xu and colleagues studied the wetting behavior and surface composition of rare earth oxides (REOs) under different post-deposition treatments in 2020;[34] they found a higher hydrocarbon concentration on a surface stored inside a vacuum chamber (1-15 Pa) for several hours compared to a surface exposed to ambient air for several months, in agreement with the aforementioned studies. However, although researchers have realized that UHV does not necessarily prevent surface contamination, relatively few studies have taken the adsorption or desorption of contaminants inside an UHV chamber into account when

conducting surface characterization under UHV,[28,30,35–37] and no prior work has studied the temporal evolution of surface composition induced by UHV systematically.

In this work, we show through experiments and physical modeling that the level of surface contamination under UHV can be described by molecular adsorption-desorption competition theory (i.e., the adsorbate on the surface approaches elemental concentration equilibrium with the surroundings). To investigate surface composition dynamics under UHV, we characterized the time evolution of surface composition under UHV in an XPS system for a period of approximately 24 hours on three gold samples, each with a different initial level of contamination. The experimental results showed good agreement with the transient adsorption-desorption model. We went on to confirm the generalizability of our results with a separate set of two 24-hour experiments conducted under UHV in another XPS system at a different location. This work provides rigorous quantitative evidence for the occurrence of both net adsorption and net desorption of VOCs under UHV, depending on the initial level of contamination, thereby offering a deeper understanding of UHV effects on surface composition; we highlight routes to mitigate these effects in sensitive experiments.

EXPERIMENTAL SECTION

Gold samples were prepared by sputtering a 560-nm-thick gold layer on a silicon substrate with an intermediate 20-nm-thick titanium adhesion layer (Figure 1a). To achieve different initial levels of contamination, we handled the gold samples in three ways: (1) one sample was cleaned under argon ion gun sputtering inside the UHV chamber where measurements were taken, and is referred to as the "in-situ cleaned" sample in the following discussion; (2) one as-deposited sample was

exposed to the ambient air for roughly 20 hours (corresponding to an incomplete, intermediate level of contamination[18]) and is referred to as the "partial contamination" sample; and (3) one as-deposited sample was exposed to the ambient air for approximately 2 weeks after sputtering deposition to attain a relatively stable level of contamination, as described in prior work,[18] and is referred to as the "stable contamination" sample. Figure 1c-d shows these pretreatment procedures.

XPS provided both the UHV environment for the experiment and the method of surface chemical composition characterization. The pressure of the XPS main chamber was maintained below 5×10^{-9} Torr. The three samples were placed into the XPS chamber at the same time and stayed inside the chamber for approximately 24 hours (Figure 1d). The atomic percentages of gold, carbon, and oxygen were measured during this period with a conventional Al Kα (1486.6 eV) X-ray source. We selected at least three individual measuring points for each sample, and the average value was adopted in the text.

We used field emission scanning electron microscopy (FEI Quanta 400 ESEM FEG; secondary electron detector used at an accelerating voltage of 15 kV) and atomic force microscopy (Park NX20) to characterize the surface morphology. Figure 1b shows the uniformity of the gold coating. The surface roughness, defined as the actual area divided by the projected surface area,[38] was determined from atomic force microscopy to be less than 1.01, indicating a nearly flat surface (Supporting Information, Figure S1).
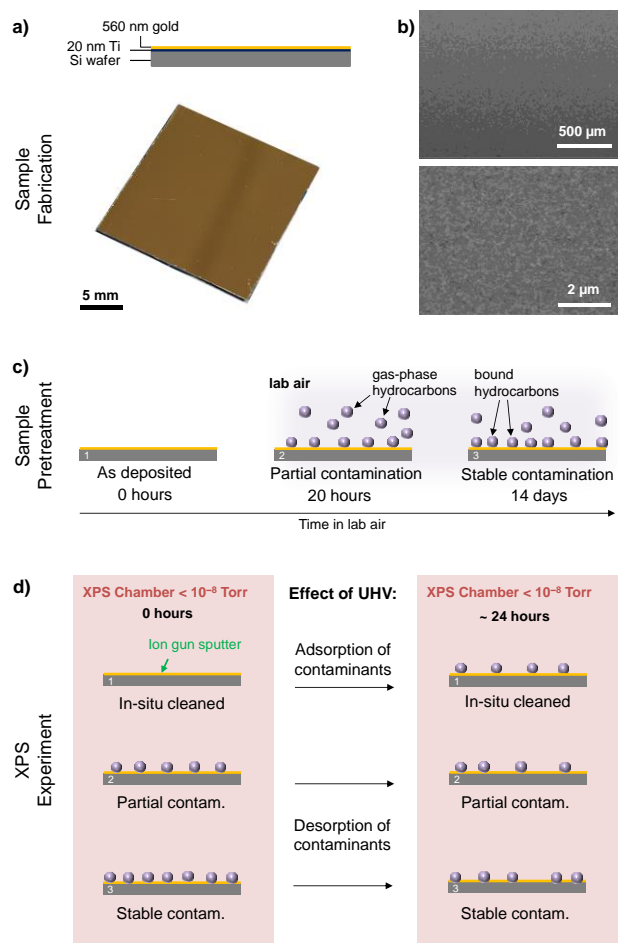
Figure 1 (Single Column). *Overview of the experiment. (a) Top panel: A schematic of the sputter-coated gold layer on a silicon substrate. Bottom panel: A photo of the actual sample after the sputtering procedure. (b) Field emission scanning electron microscope images of a gold sample, showing a smooth and uniform coating over the surface. (c) Three different pretreatments for gold samples resulting in different initial levels of hydrocarbon contamination. (d) A schematic of measurements in the XPS chamber and the observed adsorption and desorption trends.*

RESULTS AND DISCUSSION

Figure 2 shows the evolution of chemical composition of gold samples over time in the XPS chamber. Figure 2a presents the detailed C 1s XPS spectra for the in-situ cleaned sample, where

we observed a clear increase in carbon percentage over time from the area under the peak. The x-axes of Figures 2b and 2c show the residence time of samples in the UHV chamber, where initial points for the in-situ cleaned sample correspond to the state immediately after cleaning. The in-situ cleaned sample achieved 100% surface gold composition immediately after cleaning, but the carbon percentage then increased quickly over time, indicating rapid contamination. On the other hand, the partial and stable contaminated samples exhibited a decrease in carbon percentage and increase in gold percentage, implying the potential desorption of adventitious carbon from the surfaces. The loss of water molecules on these surfaces could also contribute to the observed increase in gold percentage of the contaminated samples (Supporting Information Figure S2 shows the surface oxygen evolution of three types of gold samples), but would not explain the decrease in carbon percentage. Interestingly, the surface carbon percentages of all three samples tend toward the same value (i.e., an equilibrium state) after a sufficiently long duration (~20 hours) in the UHV chamber.
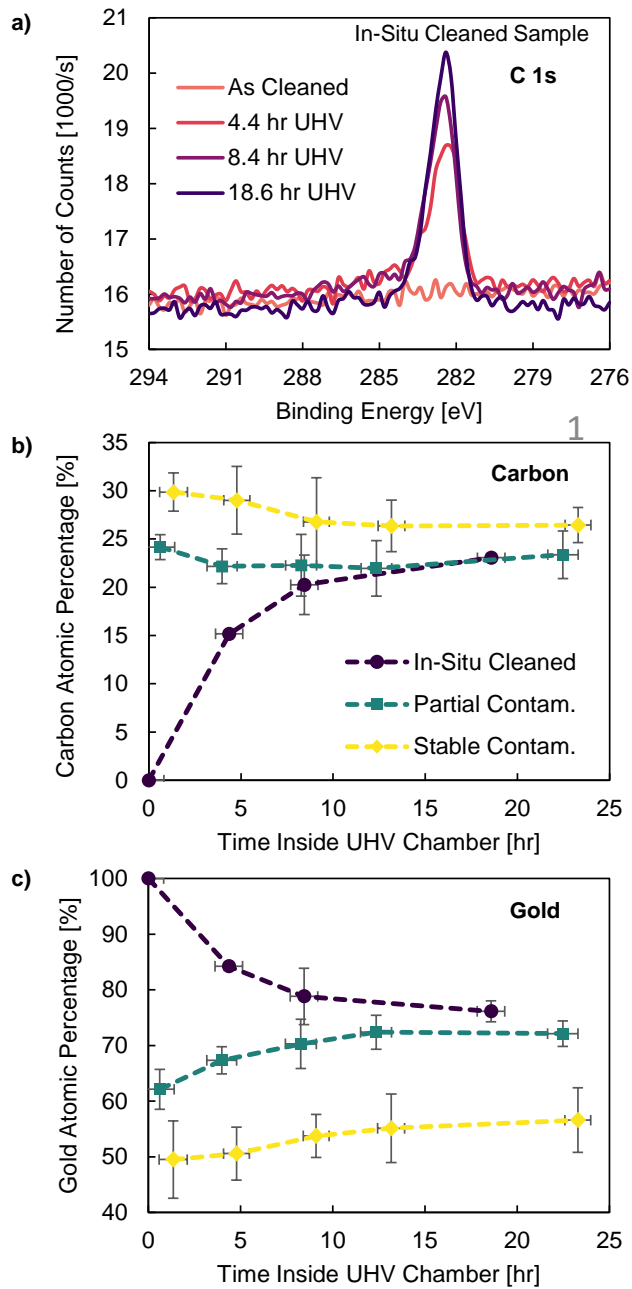
Figure 2 (Single Column). *(a) C 1s XPS spectra for the in-situ cleaned sample; atomic percentage of (b) carbon and (c) gold for three samples. The in-situ cleaned sample experienced a rapid increase of carbon percentage over time under UHV; while the two contaminated samples showed a decrease of carbon on the surface, resulting in an increase in gold concentration.*

As Figure 2 shows, the clean sample became contaminated (i.e., the carbon atomic percentage increased), while the initially contaminated samples exhibited decreases of carbon and oxygen at the surface and simultaneously reached a higher surface atomic percentage of gold over time. This time-varying surface composition phenomenon is similar to the process of hydrocarbon adsorption in ambient air. The ambient hydrocarbon adsorption process can be described by an adsorption-desorption competition model based on the Langmuir adsorption kinetic model[39] and first order desorption theory,[40] as expressed in Eq. S1 and Eq. S2 in the Supporting Information. For our gold samples inside the UHV chamber, we therefore applied a similar adsorption-desorption competition theory. Specifically, we modeled the variation of surface hydrocarbon concentration over time under UHV using Eq. 1:

$$\frac{d\varphi_s}{dt} = A - B \cdot \varphi_s \tag{1}$$

where φ_s is the hydrocarbon concentration on the solid surface, with units of number of molecules per area. A represents the adsorption rate, B is the desorption coefficient, and $B \cdot \varphi_s$ represents the desorption rate. For the adsorption rate in ambient air, A is proportional to the hydrocarbon partial pressure in the air (as suggested in Eq. S2 in the Supporting Information). Under UHV, on the other hand, A is related to the chamber conditions (such as the cleanliness of the inner chamber walls), which can be regarded as "effective hydrocarbon partial pressure," analogous to the expression of A in the air. Using a given material as a test sample, the value of A could serve as an indicator of the cleanliness for different UHV chambers.

Figure 3 shows the adsorption-desorption competition theory model results (Eq. 1) compared to our experimental data. The discrete points represent the surface hydrocarbon concentration as a function of time converted from the atomic carbon percent of the experimental data, assuming

adsorbed hydrocarbons as circular defects on the surface (Supporting Information, Figure S3b and Eq. S4). We determined the parameters $A = 8.248 \times 10^{12}$ m^{-2}·s^{-1} and $B = 6.609 \times 10^{-5}$ s^{-1} using the
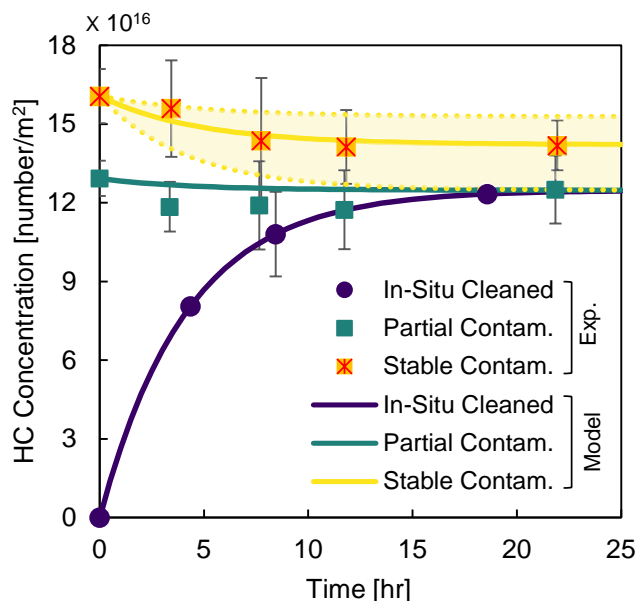

Figure 3 (Single Column). *Surface hydrocarbon concentration as a function of time for gold samples under UHV. The discrete points are converted from the carbon atomic percentage of the experimental data; the continuous lines depict the modeling results.*

least squares method[41] based on the surface hydrocarbon concentration data obtained from the in-situ cleaned sample. The dark purple solid line shows the time evolution of surface hydrocarbon concentration under UHV for the in-situ cleaned sample, indicating a good agreement between the modeling results and the data from the experiments.

Considering the adsorption and desorption mechanisms, the adsorption rate A is proportional to the effective hydrocarbon partial pressure in the chamber, while the desorption coefficient is mainly affected by the interaction between the adsorbent and the sample surface. For the three samples in our experiment, they were fabricated with the same procedure and resided in the same

UHV chamber, with the only difference being extent of initial contamination. The green solid line and yellow dashed line (lower bound) for partial contaminated and stable contaminated samples, respectively, show the model prediction when we use the same adsorption rate and desorption coefficient as the in-situ cleaned sample. The modeling results of the partial contaminated sample agree well with the data from experiment. However, the model curve for the stable contaminated sample (yellow dashed line, lower bound) deviates to some degree from the experimental data. We attribute this deviation to a potentially stronger interaction between the hydrocarbons and surfaces of the stable contaminated sample compared to the other samples, due to the formation of hydrocarbon-based multilayers (where the outermost molecules of contaminant would interact with other molecules of contaminant but not with the gold surface for highly contaminated samples), as well as dynamic composition changes from more weakly bound to more strongly bound species over time.[37] These factors result in a lower initial desorption coefficient for the stable contaminated sample; the desorption coefficient likely changes over time as some of the initial hydrocarbons are removed from the surface.

We obtained the yellow solid model curve (center line of the yellow shaded region) in Figure 3 by holding the same value of $A = 8.248 \times 10^{12}$ m^{-2}·s^{-1} (corresponding to the rate of adsorption of hydrocarbon molecules determined by the UHV chamber conditions) and fitting the desorption coefficient $B' = 5.803 \times 10^{-5}$ s^{-1}. This updated model curve agrees well with the experimental data. Because newly adsorbed hydrocarbons from the UHV chamber gradually replace the more strongly bonded initial hydrocarbons from the long-term stable contamination process, we calculated the ratio of remaining initial hydrocarbons to the total initial hydrocarbons over time assuming desorption coefficient $B' = 5.803 \times 10^{-5}$ as a constant (Figure S5 in Supporting

Information). The timescale to remove 99.9% of the initial hydrocarbons is approximately 24 hours, which is comparable to our experiment period, indicating that the variation of desorption coefficient of the stable contaminated sample is non-negligible. The fitted $B' = 5.803 \times 10^{-5}$ s^{-1} represents an average desorption coefficient during the process, while the actual desorption coefficient for the initial surface is expected to be lower. We estimated a lower desorption coefficient $B'' = 5.4 \times 10^{-5}$ s^{-1} for the initial stable contaminated surface and plotted the result as the yellow dashed line in Figure 3 (upper bound of the yellow shaded region). This model curve estimates the time-varying contamination behavior if the adsorbed hydrocarbons could remain as strongly bonded as their initial state during the entire process, while the other yellow dashed line in Figure 3 (lower bound of the yellow shaded region) suggests the tendency when the initially adsorbed hydrocarbons have the same weak bonding as the in-situ cleaned sample. Therefore, the actual time-varying surface hydrocarbon concentration of the stable contaminated sample should reside in the shaded region between the two yellow dashed curves described above; from Figure 3, we see the experimental data do indeed reside within the shaded region, supporting our hypothesis. In addition, the desorption coefficient obtained in this work has the same order of magnitude as the desorption coefficient determined from previous experimental data for hydrocarbon contamination on a gold surface in the ambient air (Table S1 in Supporting Information), which is in line with the desorption theory in the sense that desorption is mainly influenced by the solid surface properties, not the surrounding environment.

To confirm that our experimental results are generalizable and not limited to specific equipment (i.e., the XPS system at Rice University), we conducted additional experiments using a different XPS system at the Massachusetts Institute of Technology (MIT) equipped with a monochromated

Al Kα X-ray source (Versaprobe II XPS, Physical Electronics). We tested two gold samples: (i) an in-situ cleaned sample with over 99% initial surface composition of gold, and (ii) a sample that had been exposed to lab air for several days and exhibited a relatively high initial surface carbon percentage before being placed in the XPS chamber. The pressure in the XPS chamber was maintained at roughly 1.7×10^{-9} Torr. Figure 4 shows the surface carbon percentage over time in the XPS at MIT compared with the previous results obtained at Rice. We observed a similar equilibrium carbon percentage between the cleaned and contaminated samples at MIT—the carbon concentration for both samples tended toward a similar value over time. The in-situ cleaned sample at MIT exhibited a surface carbon atomic percent trend nearly identical to the sample at Rice. Likewise, the contaminated sample showed a similar desorption of surface-bound carbon-containing species. The consistent results obtained from two different XPS systems at Rice and MIT indicate that this behavior and our model are not limited to a specific environment, but can serve as a general guideline for understanding time-varying surface composition under UHV.
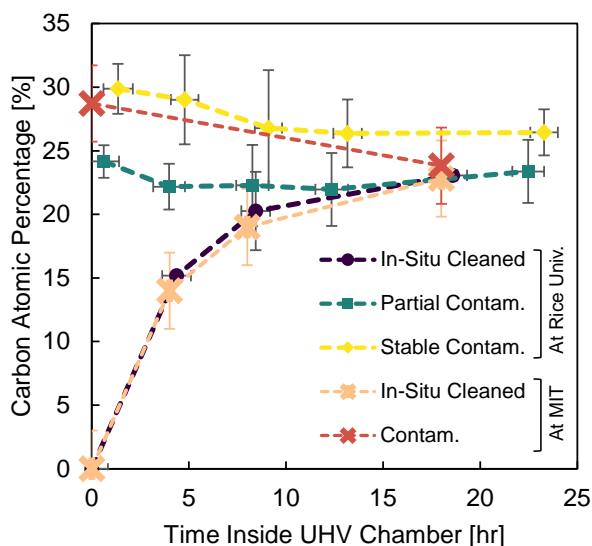

Figure 4 (Single Column). *Comparison of the evolution of carbon percentage under UHV between XPS systems at Rice University and MIT.*

Both of the two XPS systems we used in this work had vacuum levels of approximately 10^{-9} Torr. Some state-of-the-art systems with specialized requirements maintain an even higher level of UHV, for example 10^{-11} Torr in molecular-beam epitaxy and studies for space cold atom clock.[42,43] We can understand the impact of these higher levels of vacuum on hydrocarbon contamination by considering the mean free path of hydrocarbon molecules, which is already hundreds or thousands of meters in an XPS system, much larger than the scale of the XPS chamber itself. Due to the large mean free path, molecules of contaminants are not diffusing around the space within the chamber; hydrocarbons instead desorb from the solid surfaces in the chamber (inner walls, sample stage, other samples, etc.) and transport ballistically to the sample surfaces. In such a situation, solely increasing the vacuum level will not significantly affect the contamination process because the transport of contaminants will be unaffected, but the cleanliness of the chamber itself is important.

In the literature, researchers maintained clean gold surfaces over time under UHV as indicated by a near-zero water contact angle; this lack of contamination was attributed to carefully cleaning the interior of the experimental apparatus (such as baking the system for tens of hours).[44–47] By maintaining the cleanliness of the system and eliminating trace organic contaminants inside the chamber, researchers also obtained clean gold surfaces in a lower level of vacuum (10^{-6} Torr) and even at levels of pressure near atmospheric conditions.[48–50] To identify a source of contamination in our work, we characterized the surface elemental composition of the sample stage platen (which is removed from the system via a load lock device and exposed to the laboratory air while mounting samples for analysis) of the XPS system at Rice University and found that the atomic carbon

CONCLUSIONS

We characterized and modeled the transient adsorption-desorption behavior of hydrocarbons on gold surfaces under UHV. Our results indicate that the time-varying surface composition under UHV can be modeled by molecular adsorption-desorption competition theory. Initially clean gold surfaces adsorbed hydrocarbons over time under UHV, whereas initially hydrocarbon-contaminated surfaces desorbed hydrocarbons over time. During both adsorption and desorption, the concentration of contaminants tended toward the same equilibrium value.

These results suggest that residence time inside an UHV chamber can generate experimental uncertainty in surface elemental characterization techniques; therefore, experimentalists must account for the condition during storage in an UHV chamber and its influence on measurements. In order to overcome these limitations, researchers can take steps including obtaining the

measurements quickly after cleaning a surface or taking multiple measurements over time and then extrapolating the initial surface composition before contamination using our model.

Our approach was based on experimental results obtained with gold samples initially exposed to airborne contamination. Final equilibrium surface contamination levels, especially for the stable contamination samples, may have been more accurate with longer exposure to UHV, but XPS usage for longer than 24 consecutive hours proved to be impractical as XPS systems are typically shared pieces of equipment with heavily booked schedules. Future work could investigate longer times under UHV, and should also elucidate the effects of UHV for other materials with more complex elemental compositions than gold, such as metal oxides. Researchers could also probe the temporal evolution of additional species of adsorbed elements other than the atmospheric volatile organic compounds studied here. Ultimately, this study highlights a critical consideration for surface scientists, and we expect that it will serve as a guide for future work as researchers continue to elucidate these phenomena and their effects on sensitive measurements and techniques.

SUPPORTING INFORMATION

Height profile of sputter deposited gold samples from atomic force microscopy; surface oxygen evolution under UHV; modeling adsorption in a gaseous atmosphere; timescale of desorption for the stable contaminated sample under UHV; atomic carbon percentage on XPS stage platen.

AUTHOR INFORMATION

Corresponding Author

Daniel J. Preston - Department of Mechanical Engineering, Rice University, 6100 Main St., Houston, TX 77006. Email: *djp@rice.edu*

Present Address

†Lawrence Berkeley National Laboratory, 1 Cyclotron Rd, Berkeley, CA 94720

Author Contributions

Z.L. and D.J.P. conceptualized the project. Z.L., Y.S., and A.R. prepared samples. Z.L. and Y.S. conducted the experiments. Z.L. and D.J.P. developed the modeling framework. All authors analyzed the data and contributed to writing the paper.

ACKNOWLEDGEMENTS

REFERENCES

1.   Oswald S. *X-Ray Photoelectron Spectroscopy in Analysis of Surfaces*.; 2013. doi:10.1002/9780470027318.a2517.pub2

2.   Mikmeková Š, Mašek B, Jirková H, Aišman D, Müllerová I, Frank L. Microstructure of X210Cr12 steel after the forming in semi-solid state visualized by very low energy SEM in ultra high vacuum. *Appl Surf Sci*. 2013;275:403-408. doi:10.1016/j.apsusc.2012.10.139

3.   Cushman C V., Brüner P, Zakel J, et al. Low energy ion scattering (LEIS). A practical introduction to its theory, instrumentation, and applications. *Anal Methods*. 2016;8(17):3419-3439. doi:10.1039/c6ay00765a

4.   Evans L. The large hadron collider. *New J Phys*. 2007;9. doi:10.1088/1367-2630/9/9/335

5.   Hirokawa S, Teshima H, Solís-Fernández P, Ago H, Li Q, Takahashi K. Pinning in a Contact and Noncontact Manner: Direct Observation of a Three-Phase Contact Line Using Graphene Liquid Cells. *Langmuir*. 2021;37(42):12271-12277. doi:10.1021/acs.langmuir.1c01589

6.   Kothe M, Witte G. Orientational and crystalline order of copper-phthalocyanine films on gold: the role of substrate roughness and cleanliness. *Langmuir*. 2019;35(42):13570-13577. doi:10.1021/acs.langmuir.9b02658

7.   Terzyk AP, Bryk P, Korczeniewski E, et al. Water nanodroplet on a hydrocarbon "carpet" - the mechanism of water contact angle stabilization by airborne contaminations on graphene, Au, and PTFE surfaces. *Langmuir*. 2019;35(2):420-427. doi:10.1021/acs.langmuir.8b03790

8.   Hellgren N, Haasch RT, Schmidt S, Hultman L, Petrov I. Interpretation of X-ray photoelectron spectra of carbon-nitride thin films: New insights from in situ XPS. *Carbon N Y*. 2016;108:242-252. doi:10.1016/j.carbon.2016.07.017

9.   Li Z, Kozbial A, Nioradze N, et al. Water protects graphitic surface from airborne hydrocarbon contamination. *ACS Nano*. 2016;10(1):349-359.

doi:10.1021/acsnano.5b04843

10.   Hurst JM, Kim MA, Peng Z, Li L, Liu H. Assessing and mitigating surface contamination of carbon electrode materials. *Chem Mater*. 2019;31(18):7133-7142. doi:10.1021/acs.chemmater.9b01758

11.   Halim J, Cook KM, Naguib M, et al. X-ray photoelectron spectroscopy of select multi-layered transition metal carbides (MXenes). *Appl Surf Sci*. 2016;362:406-417. doi:10.1016/j.apsusc.2015.11.089

12.   Li JPH, Zhou X, Pang Y, et al. Understanding of binding energy calibration in XPS of lanthanum oxide by: In situ treatment. *Phys Chem Chem Phys*. 2019;21(40):22351-22358. doi:10.1039/c9cp04187g

13.   Not so transparent. *Nat Mater*. 2013;12(10):865. doi:10.1038/nmat3773

14.   Raj R, Maroo SC, Wang EN. Wettability of graphene. *Nano Lett*. 2013;13(4):1509-1515. doi:10.1021/nl304647t

15.   Aria AI, Kidambi PR, Weatherup RS, Xiao L, Williams JA, Hofmann S. Time evolution of the wettability of supported graphene under ambient air exposure. *J Phys Chem C*. 2016;120(4):2215-2224. doi:10.1021/acs.jpcc.5b10492

16.   Azimi G, Dhiman R, Kwon HM, Paxson AT, Varanasi KK. Hydrophobicity of rare-earth oxide ceramics. *Nat Mater*. 2013;12(4):315-320. doi:10.1038/nmat3545

17.   Khan S, Azimi G, Yildiz B, Varanasi KK. Role of surface oxygen-to-metal ratio on the wettability of rare-earth oxides. *Appl Phys Lett*. 2015;106(6):0-5. doi:10.1063/1.4907756

18.   Preston DJ, Miljkovic N, Sack J, Enright R, Queeney J, Wang EN. Effect of hydrocarbon adsorption on the wettability of rare earth oxide ceramics. *Appl Phys Lett*. 2014;105(1):1-8. doi:10.1063/1.4886410
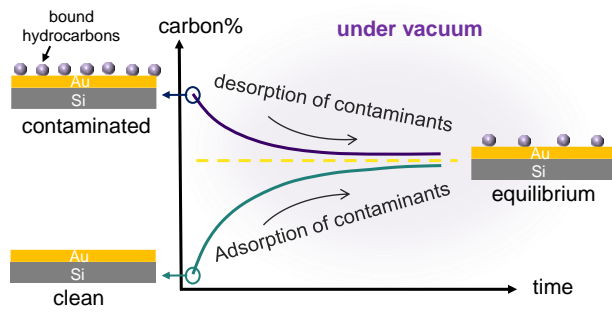
19.   Song Y, Zhang L, Liu Z, Preston DJ, Wang EN. Effects of airborne hydrocarbon adsorption on pool boiling heat transfer. *Appl Phys Lett*. 2020;116(25). doi:10.1063/5.0012839

20.   Gregorčič P. Comment on "bioinspired reversible switch between underwater superoleophobicity/superaerophobicity and oleophilicity/aerophilicity and improved antireflective property on the nanosecond laser-ablated superhydrophobic titanium surfaces." *ACS Appl Mater Interfaces*. 2021;13(2):2117-2127. doi:10.1021/acsami.9b23462

21.   Trdan U, Hočevar M, Gregorčič P. Transition from superhydrophilic to superhydrophobic state of laser textured stainless steel surface and its effect on corrosion resistance. *Corros Sci*. 2017;123(April):21-26. doi:10.1016/j.corsci.2017.04.005

22.   Chang FM, Cheng SL, Hong SJ, Sheng YJ, Tsao HK. Superhydrophilicity to superhydrophobicity transition of CuO nanowire films. *Appl Phys Lett*. 2010;96(11):2008-2011. doi:10.1063/1.3360847

23.   Takeda S, Yamamoto K, Hayasaka Y, Matsumoto K. Surface OH group governing wettability of commercial glasses. *J Non Cryst Solids*. 1999;249(1):41-46. doi:10.1016/S0022-3093(99)00297-5

24.   Takeda S, Fukawa M. Surface OH groups governing surface chemical properties of SiO2 thin films deposited by RF magnetron sputtering. *Thin Solid Films*. 2003;444(1-2):153-157. doi:10.1016/S0040-6090(03)01094-0

25.   Berman A. Total pressure measurements in vacuum technology. 1985. doi:10.1049/ep.1986.0149

26.   Pfeiffer Vacuum. *The Vacuum Technology Book - Volume II*.; 2013.

27.   White ML. Clean surface technology. In: Vol 53. ; 1973:1689-1699.

28.   Desimoni E, Casella GI, Salvi AM, Cataldi TRI, Morone A. XPS investigation of ultra-high-vacuum storage effects on carbon fibre surfaces. *Carbon N Y*. 1992;30(4):527-531. doi:10.1016/0008-6223(92)90171-R

29.   Martinez-Martin D, Longuinhos R, Izquierdo JG, et al. Atmospheric contaminants on graphitic surfaces. *Carbon N Y*. 2013;61:33-39. doi:10.1016/j.carbon.2013.04.056

30.   Landoulsi J, Genet MJ, Fleith S, et al. Organic adlayer on inorganic materials: XPS analysis selectivity to cope with adventitious contamination. *Appl Surf Sci*. 2016;383:71-83. doi:10.1016/j.apsusc.2016.04.147

31.   Long J, Zhong M, Fan P, Gong D, Zhang H. Wettability conversion of ultrafast laser structured copper surface. *J Laser Appl*. 2015;27(S2):S29107. doi:10.2351/1.4906477

32.   Jagdheesh R, Diaz M, Marimuthu S, Ocana JL. Robust fabrication of μ-patterns with tunable and durable wetting properties: hydrophilic to ultrahydrophobic via a vacuum process. *J Mater Chem A*. 2017;5(15):7125-7136. doi:10.1039/c7ta01385j

33.   Prakash S, Ghosh S, Patra A, et al. Intrinsic hydrophilic nature of epitaxial thin-film of rare-earth oxide grown by pulsed laser deposition. *Nanoscale*. 2018;10(7):3356-3361. doi:10.1039/c7nr06642b

34.   Xu P, Meng G, Pershin L, Mostaghimi J, Coyle TW. Control of the hydrophobicity of rare earth oxide coatings deposited by solution precursor plasma spray by hydrocarbon adsorption. *J Mater Sci Technol*. 2021;62:107-118. doi:10.1016/j.jmst.2020.04.044

35.   Salim M. Contamination and wettability: rare earth oxides. 2015. doi:10.1016/j.procs.2013.09.228

36.   Lundy R, Byrne C, Bogan J, et al. Exploring the role of adsorption and surface state on the

hydrophobicity of rare earth oxides. *ACS Appl Mater Interfaces*. 2017;9(15):13751-13760. doi:10.1021/acsami.7b01515

37.   Salim M, Hurst J, Montgomery M, Tolman N, Liu H. Airborne contamination of graphite as analyzed by ultra-violet photoelectron spectroscopy. *J Electron Spectros Relat Phenomena*. 2019;235(April):8-15. doi:10.1016/j.elspec.2019.06.001

38.   De Gennes, Pierre-Gilles, Françoise Brochard-Wyart DQ. *Capillarity and Wetting Phenomena: Drops, Bubbles, Pearls, Waves.*; 2013.

39.   Langmuir I. The adsorption of gases on plane surfaces of glass, mica and platinum. *J Am Chem Soc*. 1918;40(9):1361-1403. doi:10.1021/ja02242a004

40.   Redhead PA. Thermal desorption of gases. *Vacuum*. 1962. doi:10.1016/0042-207X(62)90978-8

41.   Craswell KJ. Introduction to probability and statistics. *Technometrics*. 1965. doi:10.1080/00401706.1965.10490258

42.   Mccray WP. MBE deserves a place in the history books. *Nat Nanotechnol*. 2007;2(5):259-261. doi:10.1038/nnano.2007.121

43.   Ren W, Xiang J, Zhang Y, et al. Development of an ultra-high vacuum system for space cold atom clock. *Vacuum*. 2015;116(June):54-59. doi:10.1016/j.vacuum.2015.03.001

44.   Parsegian VA, Weiss GH, Schrader ME. Macroscopic continuum model of influence of hydrocarbon contaminant on forces causing wetting of gold by water. *J Colloid Interface Sci*. 1977;61(2):356-360. doi:10.1016/0021-9797(77)90398-8

45.   Schrader ME. Ultrahigh-Vacuum Techniques in the Measurement of Contact Angles. 5. *J Phys Chem*. 1970;84(3):2774.

46.   Smith T. The hydrophilic nature of a clean gold surface. *J Colloid Interface Sci*.

1980;75(1):51-55. doi:10.1016/0021-9797(80)90348-3

47.   Gaines GL. On the water wettability of gold. *J Colloid Interface Sci*. 1981;79(1):295. doi:10.1016/0021-9797(81)90076-X

48.   Bartell, F. E. and Smith JT. Alteration of surface properties of gold and silver as indicated by contact angle measurements. 1953;57(2):165-172.

49.   Bewig KW, Zisman WA. The wetting of gold and platinum by water. *J Phys Chem*. 1965;69(12):4238-4242. doi:10.1021/j100782a029

50.   Bernett MK, Zisman WA. Confirmation of spontaneous spreading by water on pure gold. *J Phys Chem*. 1970;74(11):2309-2312. doi:10.1021/j100705a012

TABLE OF CONTENTS IMAGE

(For Table of Contents Only)